

Article

Influence of Magnesium Oxide (MgO) Nanoparticles on Maize (*Zea mays* L.)

Zain Abbas¹, Muhammad Ahmad Hassan², Weidong Huang^{1,*}, Haibing Yu¹, Mengqin Xu¹, Xiaoyu Chang¹, Xisheng Fang¹ and Liqin Liu¹

¹ College of Agriculture, Anhui Science and Technology University, Fengyang 233100, China; zainpbg47@gmail.com (Z.A.); yuhb@ahstu.edu.cn (H.Y.); xiaoxu980425@163.com (M.X.); cy410309@163.com (X.C.); fangxisheng1206@163.com (X.F.); liuliqin1206@163.com (L.L.)

² Anhui Academy of Agricultural Sciences, Hefei 230001, China; ahmaduaf93@stu.ahau.edu.cn

* Correspondence: huangwd@ahstu.edu.cn

Abstract: An approximate revolution synthesis of magnesium oxide (MgO) nanoparticles has been prepared. For plant growth and development, MgO is essential. The effect and efficiency, respectively, in seed germination, seedling growth, and plant growth were also studied. These analyses examined maize with different concentrations and parameters. The concentration of 500 ppm was tested with extreme results in areas such as plant height, protein contents both in-vivo and in-vitro, and MgO effects shown both in shoot (12.83 ± 0.5 cm) and root (5.37 ± 0.5 cm). Maximum confirmations were fixed with the help of MgO NPs characterization through TEM, SEM, FTIR, zeta potential, and X-ray. The effect of MgO NPs showed a significant increase in root and shoot length, and simultaneous in-vivo studies also showed significant results in plant physiological parameters. In effect, the vital performance in germination rate, potential, and index MgO NPs was higher than the control. Moreover, the performance and absorption of MgO NPs was confirmed by physiological characterization with the help of a UV-Vis spectrophotometer applied to the leaves and roots. It was demonstrated that the influence of MgO NPs is positive and potentially can be used for seedling growth and also for plants. It may bolster farming methods, and help maintain high food quality, quantity, and production.

Keywords: antioxidant enzymes; biochemical characterization; maize; magnesium oxide; nanoparticles



Citation: Abbas, Z.; Hassan, M.A.; Huang, W.; Yu, H.; Xu, M.; Chang, X.; Fang, X.; Liu, L. Influence of Magnesium Oxide (MgO) Nanoparticles on Maize (*Zea mays* L.). *Agronomy* **2024**, *14*, 617. <https://doi.org/10.3390/agronomy14030617>

Academic Editor: Massimo Blandino

Received: 23 February 2024

Revised: 10 March 2024

Accepted: 13 March 2024

Published: 19 March 2024



Copyright: © 2024 by the authors. Licensee MDPI, Basel, Switzerland. This article is an open access article distributed under the terms and conditions of the Creative Commons Attribution (CC BY) license (<https://creativecommons.org/licenses/by/4.0/>).

1. Introduction

Nanoparticle research is a thriving multidisciplinary area of study that is applied in many different domains [1]. While the agriculture sector has seen revolutionary improvement, innovation is still needed due to rising global food security and climate change [2]. Through better administration and maintenance of inputs to plant production, nanotechnology has the potential to significantly alter agricultural production. Using nano-fertilizers has several benefits, such as (1) particles' improved permeability into plant systems due to their nano size; (2) greater availability of reaction sites due to the high surface area available, which may increase plants' photosynthetic efficiency and increase productivity per unit of land; and (3) effectiveness of nano particles over various doses [3]. Nano-fertilizers offer sophisticated applications in plants, including accelerating chemical reactions, acting as pesticides, enhancing feed, and effectively serving as micronutrients [4]. Plants represent the main source of energy for the ecosystem and an indirect or direct influence on human life. Plant interference from insects and pathogens causes significant losses in productivity and output. Plants can be invaded by pathogens that are able to identify their attacks and react by turning on defense mechanisms [5]. There are several theories regarding how NPs work, and these theories are not entirely settled. Improved agrochemical stability, antifungal, antibacterial, and pesticidal properties, as well as advantageous effects on stress tolerance, are a few of the NP modes of action that have been discussed [6–9]. MgO

NPs present strong bactericidal action and tumor inhibition, which make them useful in a range of fields, including medicine, where they are utilized as antacids, in detoxification preparation, and in bio-molecular diagnostics [10–12]. Their use positively affects the characteristics of plant growth, such as the capacity for photosynthesis to raise chlorophyll contents, resistance to bacteria, and potential to enhance the quality of tissue culture shoots [13,14]. Common physicochemical characteristics of nanoparticles include their large surface-to-volume ratio and size structural characteristics [15]. One option in agriculture to transfer different macro- and micronutrients into the soil gradually and under control is to replace current fertilizer delivery methods with nano-fertilizers. This will prevent the accumulation and pollution of different natural resources [16]. Because nanoparticles have distinct physicochemical characteristics, they interact with plants and induce a variety of physiological and morphological changes [17].

Magnesium oxide nanoparticles (MgO NPs) are among the many different kinds of nanomaterials that can be nontoxic, accessible, and beneficial to plants [18]. As far as we are aware, a number of inorganic and organic metal oxide nanomaterials as well as a number of hybrid nanomaterials, including Fe₃O₄–Ag core shell magnetic nanoparticles, ZnO, CuO, TiO₂, and graphene oxide, are being used more frequently as alternative antibacterial agents in biomedical applications because of their unusually superior physicochemical properties, high surface-to-volume ratio, and unique nanosize structure characteristics [19–21]. MgO NPs can decrease contamination and promote the growth of plant tissue since they are more resistant to antibiotics [22]. This positively affects the growth characteristics of plants, enhancing their capacity for photosynthesis to produce higher levels of chlorophyll, increasing their resistance to bacteria, and potentially enhancing the quality of their shoot tissues [14,23,24]. To regulate the crucial biological polyphosphate molecules like ATP, DNA, and RNA, magnesium is essential. As a crucial part of chlorophyll, it plays an active role in photosynthesis and is important for plant respiration and energy metabolism. Moreover, it is a necessary nutrient for processes like protein synthesis, phloem loading, ATP synthesis in chloroplasts, carbon dioxide (CO₂) fixation, partitioning and utilization of photo assimilates, production of reactive oxygen species, and photo-oxidation in leaf tissues [24]. Since magnesium is the most restricting macronutrient in agriculture globally, it is used in this study. Furthermore, it is among the most crucial nutrients for a variety of enzyme functions as well as the structural maintenance of tissues. The significance of magnesium, which was not given much importance in the past, has been more recently realized after exploration of its vital role in cellular or enzymatic functioning. Surprisingly, nevertheless, new research has revealed that the amount of magnesium in historical cereal seeds has significantly decreased over time, and two-thirds of respondents in developed nations experience severe hypomagnesemia due to not receiving the recommended daily intake of magnesium. Therefore, two pressing practical issues are how plants respond to MGD and how to enhance the amount of magnesium in plants [25].

This study was intended to assess the effects of magnesium oxide nanoparticles, or MgO NPs, on maize seed germination and growth both *in vitro* and *in vivo*. We looked at how nanoparticles affected the morphology of plants, including the length of the shoots and roots, and physiological characterization. To assess the translocation of magnesium in maize (*Zea mays* L.), the magnesium content in several plant sections was also determined with size and shape visualization. This work is the first that we are aware of that offers a thorough analysis of how nanoparticles positively affect the growth of *Zea mays*.

2. Materials and Methods

This study used *Z. mays* (maize genotype) collected from the Anhui Science and Technology University. Additional chemicals, like sodium oxide (NaOH) and magnesium oxide (Mg(OH)₂), were bought from Hi-media Pvt. Ltd., in Shenzhen, China and used without additional purification. At room temperature, the MgO NP was synthesized at Anhui Science and Technology University via a colloidal technique [26]. The particles were 20 nm in diameter. Gui hua (*Osmanthus fragrans*) leaves were collected from the garden

of Anhui Science and Technology University. The magnesium precursor was magnesium nitrate hexahydrate $\text{Mg}(\text{NO}_3)_2 \cdot 6\text{H}_2\text{O}$ (98%).

2.1. Leaves Extract and MgO NP Synthesis

Distilled water was used to wash fresh Gui hua (*Osmanthus fragrans*) leaves to remove dirt and contaminants. The sanitized and dried leaves were then cut into smaller pieces and brought to a boil for 20 min at 90 degrees Celsius using purified water. Next, filter paper was used to filter the leaf extract. A total of 9.1 M of magnesium nitrate hexahydrate was dissolved in 350 mL of distilled water. Then, Gui hua (*Osmanthus fragrans*) leaf extract was progressively added dropwise into the solution with steady mixing for 20 min at 80 °C. Once precipitate appeared, we checked the pH, ensuring it was between 7 and 8. After centrifuging the solution for 15 min at 5000 rpm, we collected the extract and heated it for two hours at 72 to 80 degrees Celsius, then let it sit at 100 degrees for two days. Finally, we collected the powder and ground it using a pestle and mortar. The process is shown in Figure 1.

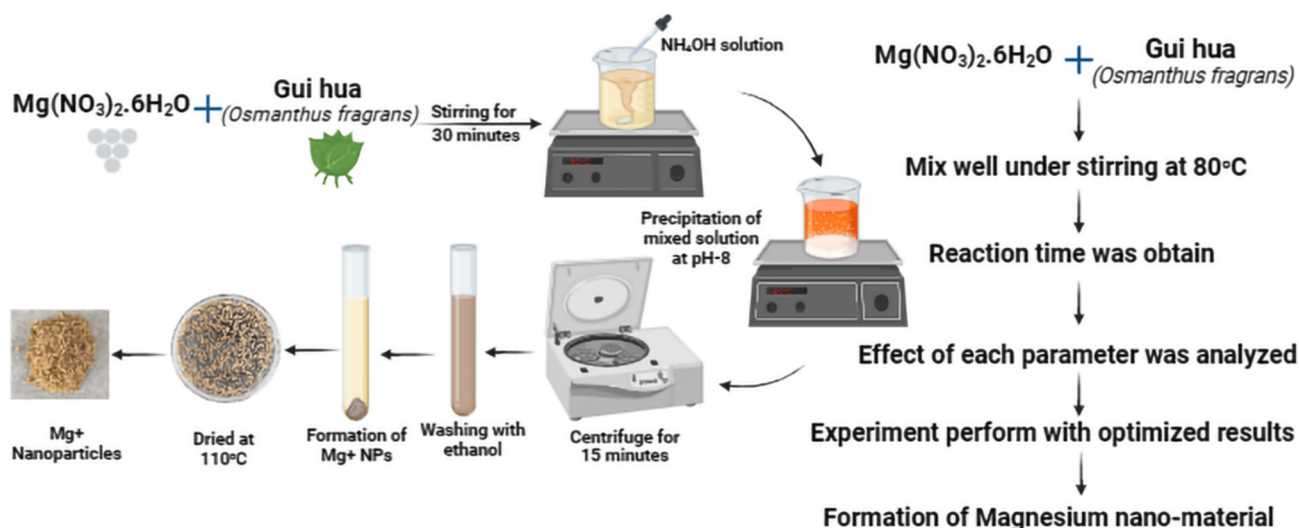


Figure 1. Preparation process of magnesium nanoparticles (MgO NPs).

2.2. Composition of Magnesium Nano-Material

Next, the MgO nano-materials were thoroughly characterized using TEM (transmission electron microscopy), SEM (scanning electron microscopy), XRD (X-ray diffraction), FTIR (Fourier-transform infrared spectroscopy), zeta potential, TG (thermogravimetry), and other analytical tools to gather data on shape, particle size, particle size distribution, crystalline state, surface groups, surface charge, dispersion, etc. The nano-magnesium was prepared using biological methods.

The MgO nanoparticles were spread by ultrasonic vibration (250 W, 20 kHz) after being directly suspended in pure water for 30 min by ultrasonic means. Suspensions containing CK (control), 100 ppm, 200 ppm, 500 ppm, 800 ppm, and 1000 ppm of nanoparticles were prepared.

2.3. Seed Germination Exposure

The seeds were suspended in double-distilled water to test their viability. The seeds that sank to the bottom were chosen for additional investigation. After three rounds of rinsing in double-distilled water, the seeds were surface-sterilized. After 10 min in 0.1% mercuric chloride, three rounds of washing were conducted with sterile distilled water. On sterile cotton beds in each sterile petri plate, five sterile seeds were inserted (in triplicate for each treatment listed below). Whitman filter paper No. 1 was placed on the sterile cotton to prepare the cotton bed, and sterile distilled water was added to preserve moisture. After

30 min of sonication, the biologically produced MgO nanoparticles were added to prepared nanoparticle solutions (0.0, 0.5, 1.0, and 2.5 mg/50 mL) containing the sterile seeds, which were then soaked and placed in prepared pots to be observed for growth.

Seed Germination Percentage

The counts were made following ISTA guidelines from 1993 and were reported as a percentage. The following equations were used to determine the root growth (RG), the seed germination rate (GR), and the germination index (GI).

$$\text{Germination Rate} = (Sc/Ss)100$$

$$\text{Root Growth} = (Rs/Rc)100$$

$$\text{Germination Index} = (GR/RG)100$$

Here, Ss is the number of seeds that germinated in the sample. Sc is the number of seeds germinated in control. Rs is the average root length in the sample, and Rc is the average root length in the control. The measurement of the root's length was made from the section below the hypocotyls to the tip. Shoot length was measured starting at the base of the cotyledons and moving up to the base of the root–hypocotyl transition zone. Scale was used to measure the lengths of the roots and shoots.

The seedling growth index was measured by using this formula:

$$\text{SGI} = (\text{ARL}/\text{ASL}) \text{GP}$$

Here, SGI is the seedling growth index, ARL is average root length, ASL is average shoot length, and GP is germination percentage.

2.4. Seedlings Growth in a Greenhouse

The research study was conducted in two ways. In the first experiment, seeds germinated in the control condition at 26 ± 2 °C for three days. The three-day-old seed with emerging radicle-like seedlings was hardened into pots with three replications for each concentration. In the second experiment, seeds were germinated in control conditions at 26 ± 2 °C for seven days. The seven-day-old seed with emerging radicle-like seedlings was hardened into pots with three replications for each concentration. After the germination, the nanoparticle suspension was sprayed with designed concentrations for each replication after 7 days (1 mL of each concentration of nanoparticle to every plant leaf).

2.5. Plant Growth in the Field

To further study the efficiency of synthesized nanoparticles, a proper field was prepared for this experiment. Seed was then sown manually on ridges with the help of a seed driller. Different sets of plants were maintained in triplicate for each treatment of nanoparticles in ppm 100, 200, 500, and control. Ten plants were chosen for each concentration of nanoparticle from the middle of the field after one month of growth. Every plant was labelled with number, concentration, and replication. After the maximum growth of the plant, the nanoparticle suspension was sprayed on leaves with designed concentrations (100, 200, 500) for each replication after seven days (5 mL of each concentration of nanoparticle to every plant leaf). Following 60 days of the experiment, measurements were made of the root length, fresh weight (the average of the five plants' weights), and dry weight (the average of the five plants' weights). The data collected on the sixty-first day of the experiment were taken into consideration for analysis in this study.

3. Results

Using Gui hua (*Osmanthus fragrans*) filtrate, the modified co-precipitation approach was utilized to synthesize MgO NPs. The production of MgO NPs was shown by the development of a white precipitate at pH 8. Chemical synthesis was the method for

producing magnesium oxide nanoparticles, or MgO NPs [27]. This method is the biological method [28,29].

3.1. Characterization of Synthesized MgO NPs

The scanning electron microscopy (SEM) image analysis forecasts the morphology and production of stable MgO nanoparticles produced by the present green method [30]. The majority of the MgO NPs showed uniform aggregation, with an average particle size distribution range of 5 nm Figure 2I. The polydispersed nanoparticle production was verified by the TEM micrographs [30]. It was discovered that MgO NPs ranged in size from 30 to 100 nm Figure 2II.

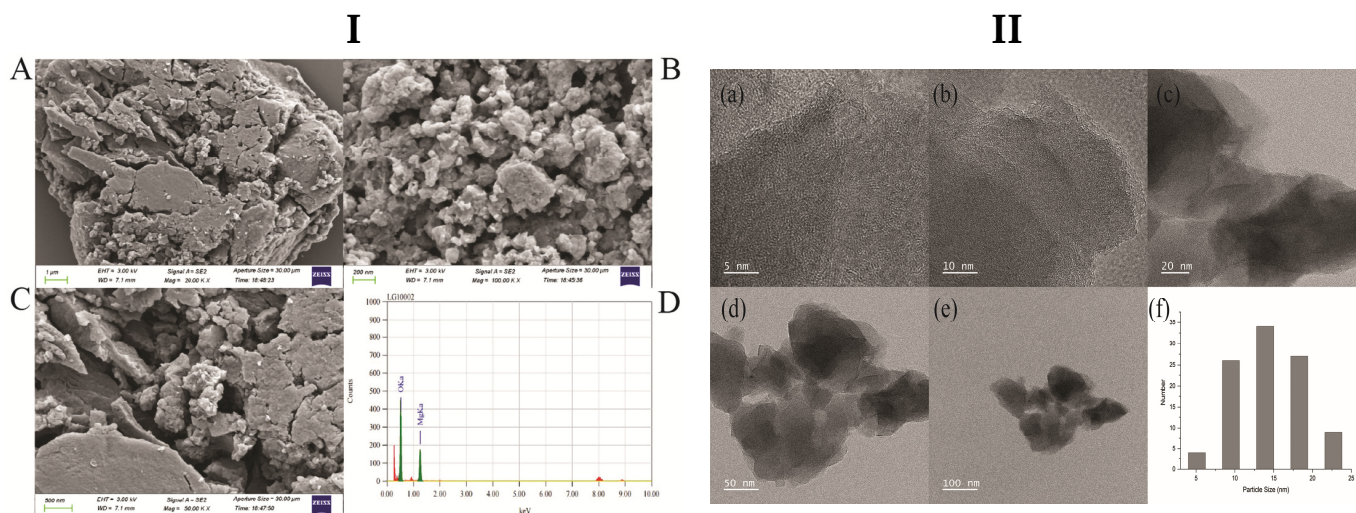


Figure 2. (I) SEM analysis of MgO nanoparticles, (A) NPs stability at 1 μm . (B) 200 μm , (C) 500 μm , (D) stability level graph. (II) TEM analysis of MgO nanoparticles, (a) range of NPs size at 5 nm, (b) 10 nm, (c) 20 nm, (d) 50 nm, (e) 100 nm and (f) NPs size graph.

The FTIR (Figure 3A) spectra of the generated magnesium nanoparticles showed curves at 3701.20, 3419.65, 1630.74, 1496.73, 1384.30, 1047.99, and 567.93 cm^{-1} of the sample. The FTIR spectra obtained for fungal filtrate displayed absorption bands at 1630.74 cm^{-1} , 1047.99 cm^{-1} , and 567.93 cm^{-1} , which correspond to N–H bond, CH₃–CH₃ bonding and C–N stretch, respectively. The different functional groups (Figure 3B) found in biomolecules (proteins) that these absorption peaks correlate to may aid in the boosting of ions to nanoparticles [31]. There are many applications on a single diffractometer platform with intensity set to 592 at 38 degrees and 298 at 59 degrees [32,33]. It was discovered (Figure 3C) that the zeta potential of MgO NPs was -13.9% mV, even though the zeta potential values were between -25 and $+25$ mV. The first of these two curves occurs (Figure 3D) at 253.91 $^{\circ}\text{C}$ and reduces mass loss by 10.084%. At 415.16 $^{\circ}\text{C}$, the second curve reduced mass loss by 28.53% in thermogravimetry (TG).

3.2. Effect of MgO NPs on *Z. mays* Seed Germination

Our observations indicate a considerable increase in the germination rate of *Z. mays* seeds following treatment with MgO NPs. The data of different replications and each replication count with total 50 seeds for germination test measured (Table 1). Among the treatments using different MgO NP concentrations (i.e., CK, 100, 200, 500, 800, 1000 ppm), treatment of the seeds with 500 ppm resulted in the highest GP. However, decreased GP was present in the control group, which consisted of treated seeds that were not given any MgO NP treatments.

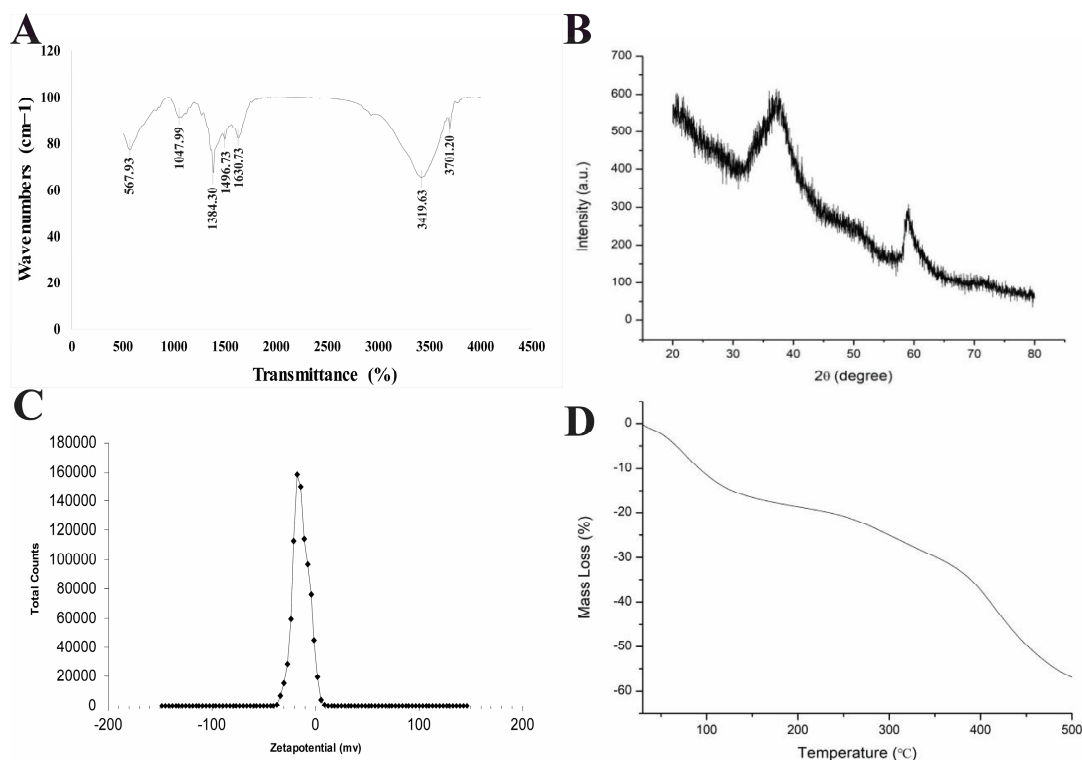


Figure 3. (A) FTIR (Fourier-transform infrared spectroscopy), (B) XRD (X-ray diffraction), (C) zeta potential and (D) TG (thermogravimetry) characterization of MgO NPs.

Table 1. 7th Day Seed germination percentage.

Treatments	R1 (cm)	R2 (cm)	R3 (cm)	GS (Numbers)	GP (%)
CK	11	14	16	41	27.33
100 ppm	18	22	16	56	37.33
200 ppm	25	27	21	73	48.67
500 ppm	34	45	46	125	83.33
800 ppm	16	22	12	50	33.33
1000 ppm	14	12	18	44	29.33

Note: Treatments: in parts per million; R: replications; GS: no. of grown seeds; GP: germination percentage.

In addition to these characteristics, it was found that in comparison to untreated seeds, seeds treated with different doses of MgO NPs showed a considerable increase in shoot height and root length, as shown in Figure 4. For the maximum treatment of 500 ppm of Mg(OH)₂ NPs, measurements were taken of shoot height (10.4 ± 0.3 cm) and root length (19.1 ± 0.6 cm).

The results above clearly expressed that MgO NPs positively impacted shoot and root development in addition to having a significant impact on all seed germination parameters. As of right now, however, there is no concrete evidence to back up the theory that MgO NPs cause seed germination in maize. It is plausible that Mg(OH)₂ NPs adhere to the waxy coating found on *Z. mays* seeds, and that their nano size allows them to pass through the seed coat and positively impact the germination process, as seen in Figure 5.

Beneficial impacts of MgO NPs are as follows during the seed germination. (1) Seeds' ability to absorb water and nutrients is increased by nanoparticles. (2) Water is quickly absorbed by seeds, which solubilizes the gibberellic acid (GA) in the embryo and travels to the seed tissue and aleuronic cytoplasm, where it activates the central dogma system and generates the enzyme amylase. Additionally, the enzyme amylase converts seed starch into sugars and gives the seed cells the energy they need to germinate. (3) By helping to raise

the amount of nitrate reductase in the embryo, nanoparticles aid in the promotion of seed germination and antioxidant systems by improving the ability of the seeds to absorb and use water and other nutrients. (4) By lowering H_2O_2 and superoxide radicals, nanoparticles contribute to the decrease of oxidative stress and improve the activity of important enzymes involved in seed germination [24].

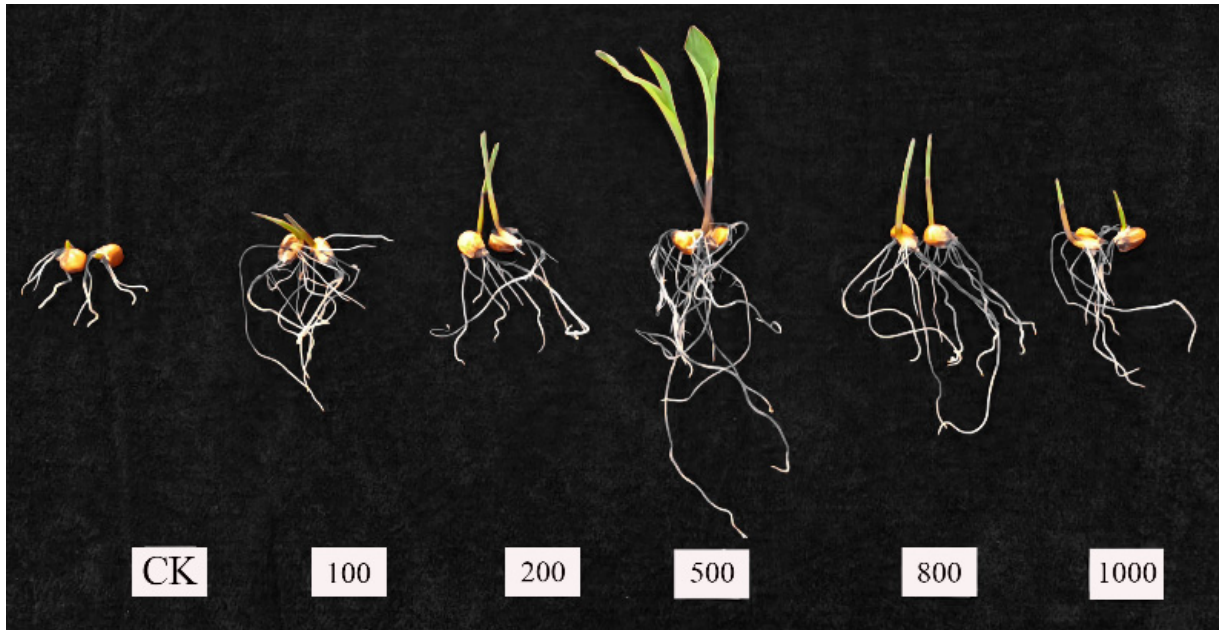


Figure 4. Effect of MgO NPs on seed germination by seventh day with different concentrations CK, 100 ppm, 200 ppm, 500 ppm, 800 ppm, and 1000 ppm.

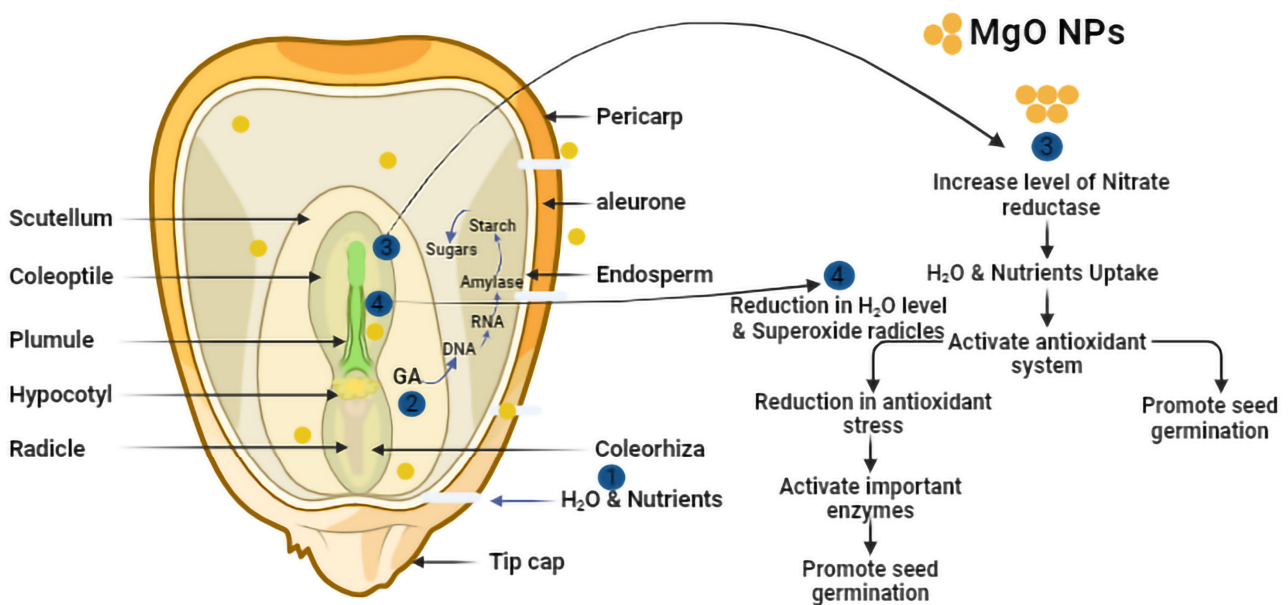


Figure 5. Schematic illustration of potential theoretical processes in *Zea mays* seed germination in the presence of MgO NPs.

3.3. Efficacy of MgO NPs on Seedling Growth in Greenhouse

To find the effect MgO NPs on *Z. mays* seedlings, we chose performance concentrations including control, 100 ppm, 200 ppm, and 500 ppm. The maximum 500 ppm shoot height (60.3 ± 0.3 cm) and root length (35.2 ± 0.6 cm) were measured. The maximum 200 ppm

shoot height (54.1 ± 0.3 cm) and root length (26.7 ± 0.6 cm) were measured. The maximum 100 ppm shoot height (47.4 ± 0.3 cm) and root length (18.2 ± 0.6 cm) were measured. The maximum control ppm shoot height (40.7 ± 0.3 cm) and root length (15.4 ± 0.6 cm) were measured. We also tested for seed germination rate (GR), germination potential (GP), and germination index (GI), in an effort to broaden the experiment. The finding of these testes appeared to support 500 ppm concentration. The Table 2 presents the results below.

Table 2. Seed germination rate, germination potential, and germination index.

Treatments	Germination Rate (%)	Germination Potential (%)	Germination Index (%)
CK	40.67	20.33	8.74
100 ppm	48.67	24.33	10.43
200 ppm	58.12	29.37	12.43
500 ppm	75.33	37.67	16.15

Note: Data collected after one month of spray on maize seedlings.

3.4. Effect of MgO NPs on Maize Plants' Growth

In light of the encouraging results of MgO NPs with regard to seed germination and seedling growth and plant growth Figure 6, we next conducted a field investigation to assess the effectiveness of these nanoparticles in promoting plant growth for three months. The measurements were made on the basis of morphological traits such as plant height and root length. We selected some plants for control and some for the other concentrations.

The biophysical phenotyping methodology has a directly proportionate effect, as seen in Figure 7 [34] illustrate, As the concentration approach 500 ppm the results reveal an increase. Following treatment of the plants with varying MgO NP concentrations (100, 200, 500, 800, and 1000 ppm), 500 ppm was dominant, as shoot height (240.4 ± 1.6 cm) and root length (129.2 ± 1.3 cm) significantly increased after 120 days. In comparison, the plants treated with control showed inadequate growth and development, with plant height of 205.6 ± 2.3 cm and root length 89 ± 1.5 cm.

Effects of MgO NPs on Maize Plant

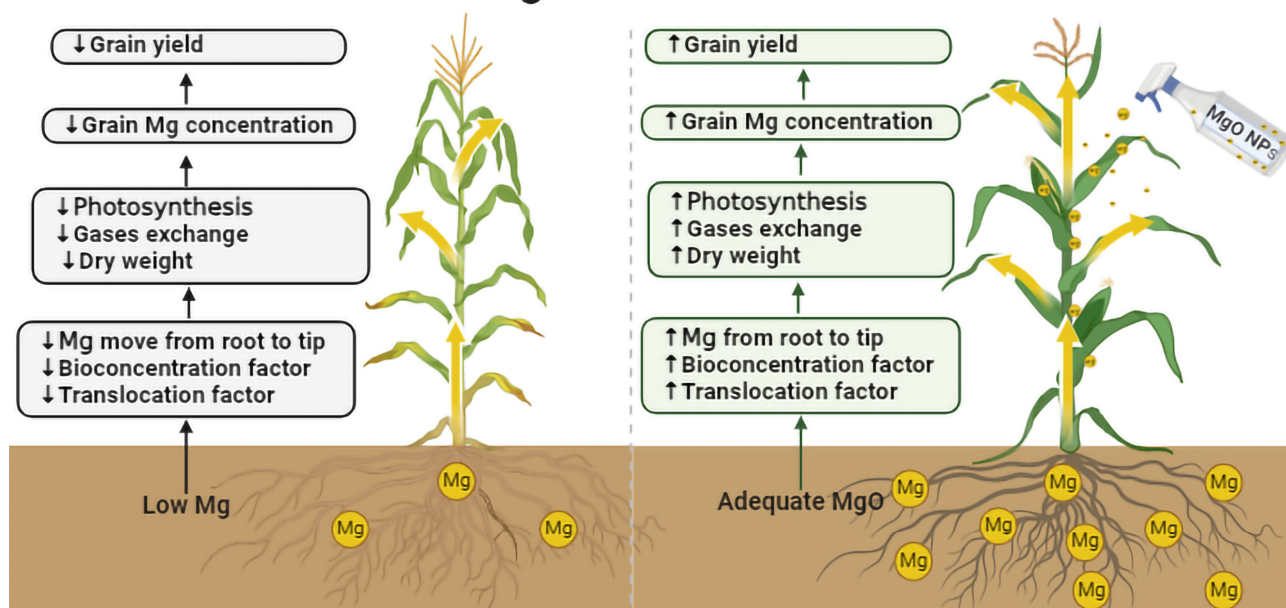


Figure 6. Effect of MgO NPs on maize plant growth.

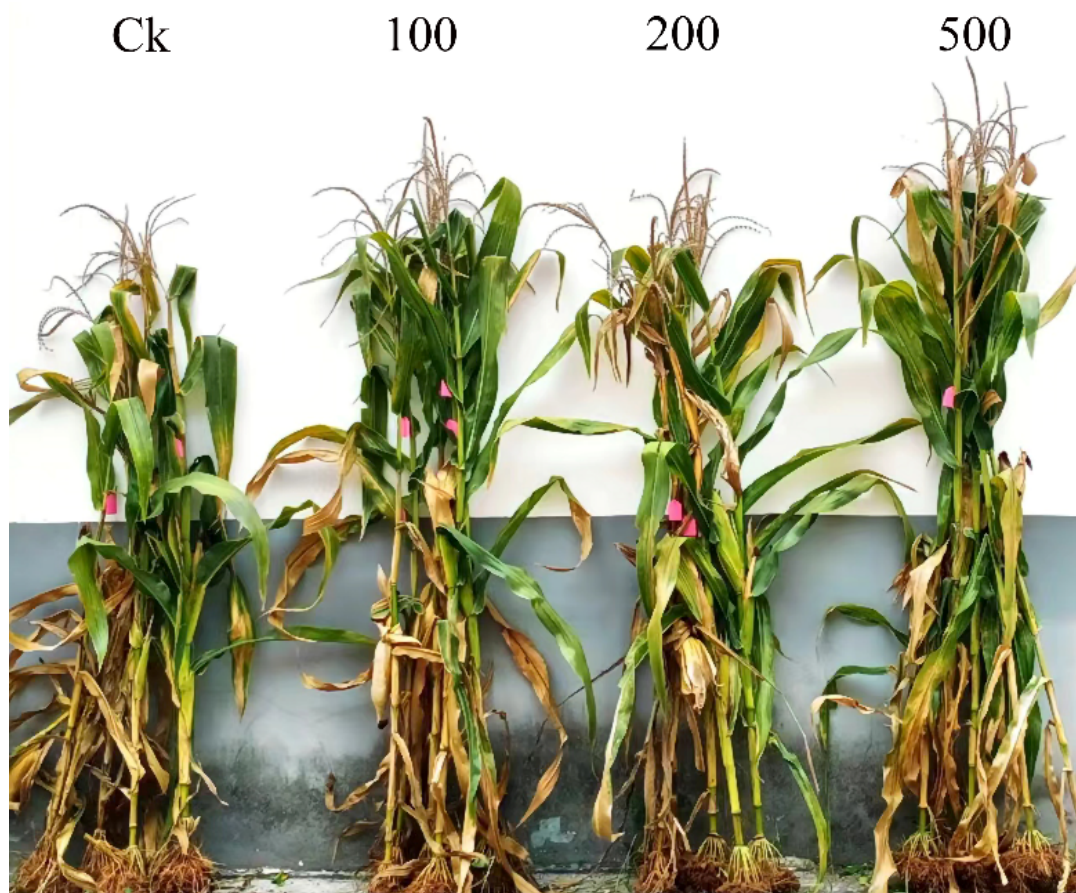


Figure 7. Phenotypic effect of MgO NPs on maize plant growth.

3.5. Biochemical Characterization of Maize Treated with MgO NPs

3.5.1. Antioxidant Enzymes

The activity of an organism's internal enzymes is generally directly connected with its capacity to tolerate adversity [35]. Antioxidant enzymes such as SOD, POD, CAT, and PPO scavenge O_2 to safeguard the plant's internal enzyme system and improve response time in shoots and roots. The SOD activity was significantly higher in 500 ppm-treated seedlings. Plant material (leaf and roots) was collected and freeze-dried to maintain integrity. Extraction was performed using appropriate solvents (e.g., methanol, ethanol).

Activity of the SOD antioxidant enzymes in shoots of CK was 11.5%, and 62.4% at 500 ppm concentration. In CK roots, SOD was 9.3%, while it was 32.3% at 500 ppm concentration (Figure 8A). The PPO antioxidant enzymes in shoots of CK was 32.2%, and 56.2% at 500 ppm concentration. PPO in CK roots was 28.8%, and 62.7% at 500 ppm concentration (Figure 8B). The CAT antioxidant enzyme activity in shoots of CK was 54.24%, and 76.28% at 500 ppm. In CK roots, CAT was 20.56%, while at 500ppm it was 68.82% (Figure 8C). The POD antioxidant enzyme activity in shoots of CK was 20.21%, and 92.12% at 500 ppm. In CK roots, POD was 30.16%, while at 500 ppm it was 85.32% (Figure 8D). The results obtained with CK were not good as accepted.

3.5.2. Membrane Lipid Peroxidation

Lipid peroxides are created when oxygen-derived free radicals react with unsaturated fatty acids in lipids. These enzymes include MDA, H_2O_2 , O_2^- , protein, soluble sugar, and total phenol [36]. We used a 1:5 ratio of extract liquid volume to tissue weight, following the recommendation of weighing about 0.1 g of sample and adding 1 ml of extract liquid. The extraction process was performed with ice bath homogenization. After centrifuging the mixture 8000 rpm for 10 minutes at 4 °C, collected the supernatant and placed it on ice

for further measurement. Spectrophotometer was preheated for at least 30 minutes. The wavelength was set at 525 nm. Measurement were taken using reagent 1 (distilled water) and reagent 2 (sample). Both preheated for more than 10 minutes at 37 °C [37]. The MDA contents were 0.24% in shoots of CK and 0.54% at 500 ppm. Roots were 0.21% for CK and 0.44% at 500 ppm (Figure 9A). The H₂O₂ content in shoots of CK was 0.039%, and 0.097% at 500 ppm. In roots, it was 0.041% for CK and 0.061% at 500 ppm (Figure 9B). The O₂⁻ contents in shoots of CK was 0.763%, and 1.423% at 500 ppm. In roots, it was 0.625% for CK and 1.059% at 500 ppm (Figure 9C). The soluble sugar content in shoots of CK was 0.412%, and 1.187% at 500 ppm. In roots, it was 0.247% for CK and 0.882% at 500 ppm (Figure 9D). The protein content in shoots of CK was 0.404%, and 0.907% at 500 ppm. In roots, it was 0.325% for CK and 0.812% at 500 ppm (Figure 9E). The total phenol content in shoots of CK was 11.45%, and 14.43% at 500 ppm. In roots, it was 10.85% for CK and 13.12% at 500 ppm (Figure 9F).

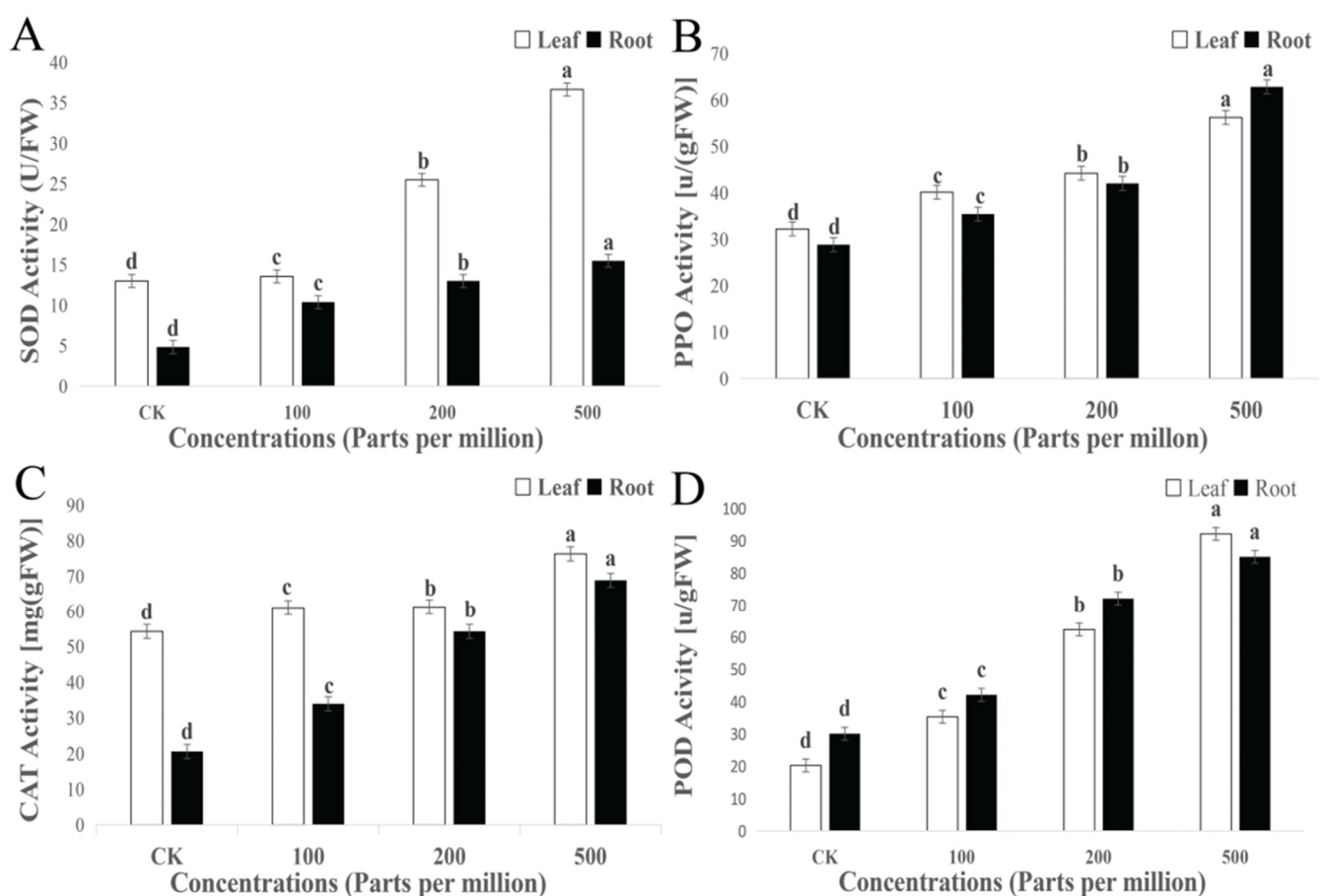


Figure 8. Effects of different concentrations of MgO on antioxidant enzymes, (A) the effect of SOD activity, (B) PPO activity, (C) CAT activity and (D) POD activity. Here the a means highest content level and b, c and d are lowest content level respectively.

3.5.3. Plant Defense Enzymes

Phenylalanine ammonia lyase (PAL) is present in many different types of plants as well as a small number of microorganisms. It is crucial for the healthy growth and development of plants as well as their ability to fend off infections [38]. Activity of plant defense enzymes such as catalase, peroxidase, and superoxide dismutase was determined by spectrophotometer using standard assay protocols [39]. The PAL activity in shoots of CK was 26.82%, while it was 54.32% at 500 ppm. In roots, it was 41.87% for CK and 73.0% at 500 ppm (Figure 10).

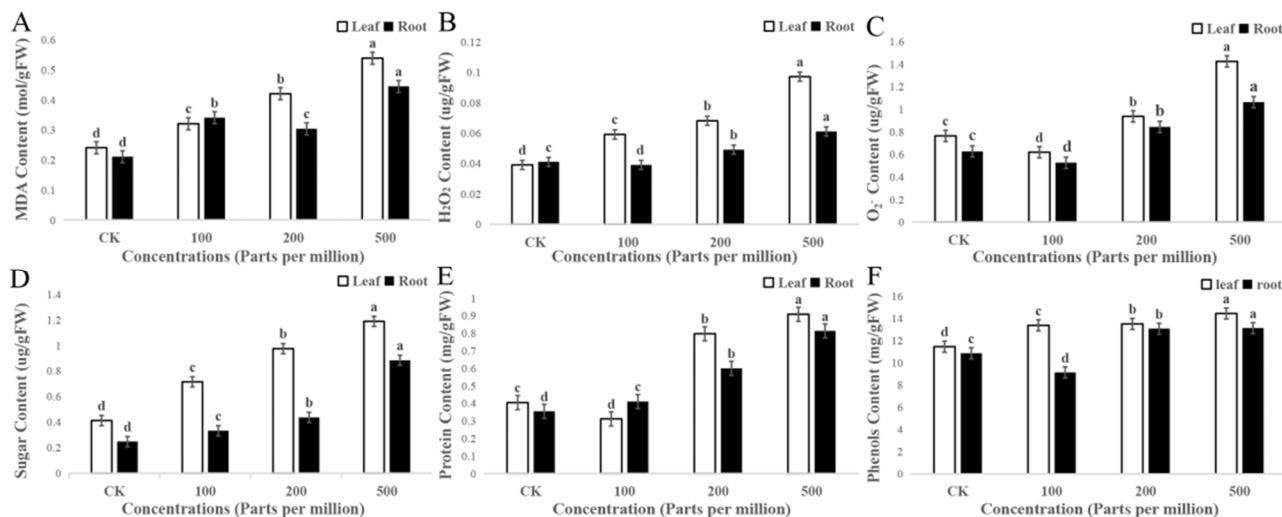


Figure 9. Effects of different concentrations of MgO, (A) MDA, (B) H₂O₂, (C) O₂⁻, (D) sugar, (E) Protein, (F) phenol content activity on membrane lipid peroxidation. Here the a means highest content level and b, c and d are lowest content level respectively.

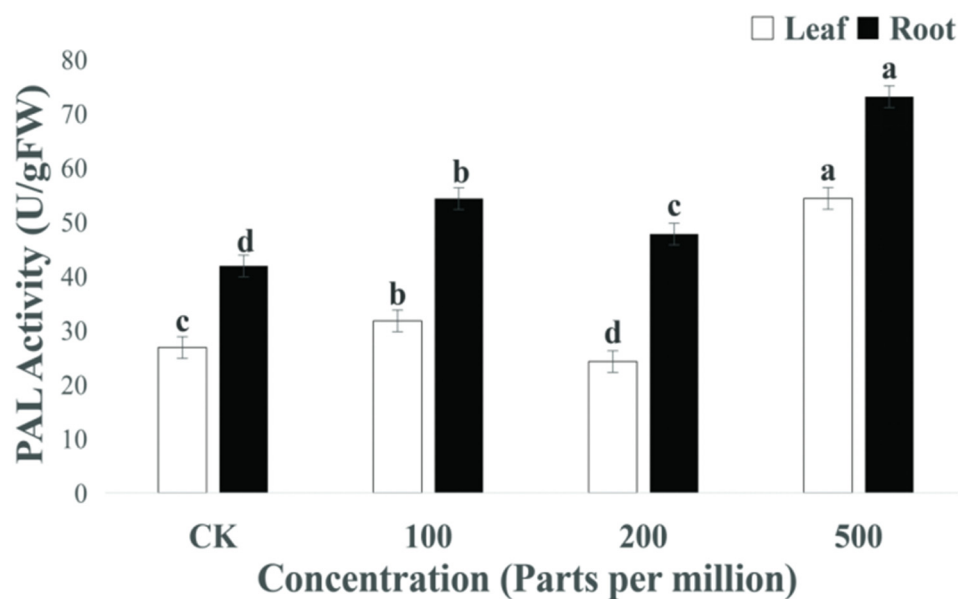


Figure 10. Effects of different concentrations of MgO on plant defense enzymes. Here the a means highest content level and b, c and d are lowest content level respectively.

3.5.4. Phenolics

Tannin is a type of polyphenol compound known to interact with various metal ions through complexation or electrostatic action. Additionally, it has been observed to contribute to hemostasis and inhibit the growth of microorganism [40]. For analyzing tannins and flavonoids, it is recommended to weigh about 0.1 g of leaf and add 1 mL distilled water, fully homogenize, and transfer to EP tube, sealing the film to prevent liquid spatter. The mixture is then extracted at 80 °C and placed in a water bath for 30 min. This is followed by 10 min in an 8000 rpm centrifuge at 25 °C, and finally the supernatant is removed to be measured. A spectrophotometer is preheated for more than 30 min, the wavelength is adjusted to 760 nm, and measurement is taken with reagent 1 (distilled water) and reagent 2 (sample) preheated for more than 10 min at 37 °C [41]. The tannin content was 18.17% in shoots of CK and 56.89% at 500 ppm. In roots, it was 35.64% for CK and 66.78% at 500 ppm (Figure 11A). Flavonoids are a kind of polybenzene compound. In an alkaline

nitrite solution, flavonoids and aluminum ions form a red complex with characteristic absorption [42]. Flavonoid content was 3.39% in shoots of CK and 3.65% at 500 ppm. In roots, it was 2.21% for CK and 2.87% at 500 ppm (Figure 11B). The 500 ppm treatment consistently outperformed the control in both tannins and flavonoids.

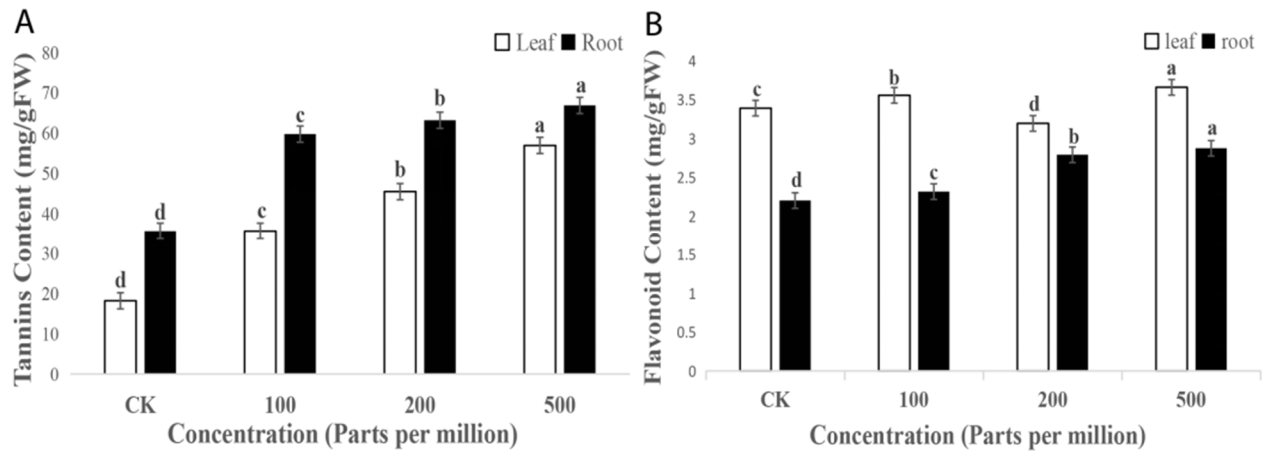


Figure 11. Effects of different concentrations of MgO on phenolics. Here the a means highest content level and b, c and d are lowest content level respectively.

3.5.5. Acetylcholinesterase (AChE) Activity

Acetylcholinesterase (AChE) is a serine hydrolase. It catalyzes the hydrolysis of acetylcholine (ACh) to form choline, and choline reacts with DTNB to form 5-mercapto-introbenzoic acid (TNB) [43]. To access the activity of acetylcholinesterase (AChE), Begin by grinding 0.1 g of leaves and adding 1 ml of extract liquid in an ice bath for homogenization. Next, Centrifuge the mixture at 8000 rpm for 10 minutes at 4 °C. after preheating a spectrometer for 30 minutes, adjust the wavelength to 412 nm. The reagent 1 (distilled water) and reagent 2 (sample). Both preheated at 37 °C before 10 minutes [44].

AChE activity was 4.45% in shoots of CK and 23.41% at 500 ppm. In roots, it was 6.93% for CK and 14.71% at 500 ppm (Figure 12). AChE also reaches its maximum at the 500 ppm concentration. Thus, the results of all the experiments characterizing MgO NPs, with regard to seed germination (%), seedling growth (GR, GP, GI), and plant growth, show in favor of the 500 ppm concentration.

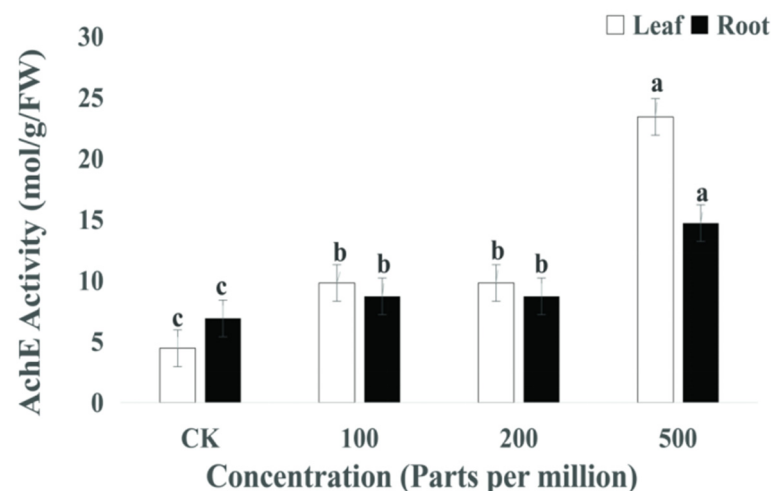


Figure 12. Effects of different concentrations of MgO on acetylcholinesterase activity, Here the a means highest content level and b and c are lowest content level respectively.

4. Discussion

4.1. Physical and Chemical Properties of MgO NPs

It is well known that various chemical reactions occur during the penetration of foreign nanoparticles into the seed and leaves [45]. To understand the possibility of the maximum influence of nanoparticles, we performed SEM. The resulting numbers attest to the high level of nanoparticle stability. Ultimately, the size and shape of MgO NPs were ascertained using transmission electron microscopy (TEM). The FTIR spectra of the produced magnesium oxide nanoparticles, as well as bioactive compounds that might be related to the chemical synthesis of the particles and their stability, were investigated. Moreover, the FTIR spectrum reported for MgO NPs showed absorption bands at 1496.733 cm^{-1} due to $-\text{C}\equiv\text{C}-$ stretch, and $34,199.65\text{ cm}^{-1}$ and 1384.30 cm^{-1} due to stretching of C–N [46–48]. To look into the phase and purity of the manufactured MgO NPs, the XRD patterns were captured. XRD is the only laboratory technique that accurately and non-destructively gathers data on things like layer thickness, preferred orientation, lattice strain, crystal size, and chemical composition. Encapsulating biomolecules like proteins over nanoparticles during biological synthesis has an impact on the zeta potential value [49]. Using simultaneous thermogravimetry (TG), the thermal properties of the investigated heterocyclic esters were ascertained [50]. In an air-filled atmosphere, it was observed that all of the compounds were thermally stable and that their thermal stability increased with changes in mass during heating [51].

4.2. Morphological Changes in Germination

We investigated the germination efficiency of MgO NPs at different doses. A number of seed germination-related metrics were examined, including mean germination rate (GR), germination index (GI), and germination potential (GP). The percentage of germination for each day of the germination phase is expressed by the GI. Greater and faster seed germination is indicated by higher GI values. As compared to the control group (untreated seeds), the findings show the influence of concentration on seed germination. No such study using MgO NPs has been conducted previously. The authors of a prior work showed that MgO NPs had a concentration-dependent influence on *Z. mays* seed germination [52]. According to a different study, MgO nanoparticles can successfully pierce the seed coat and affect seed germination [53]. Seeds treated with different doses of MgO NPs have been shown to significantly increase growth of shoots and roots. Other researchers have shown a positive impact from the function of nanoparticles, such as titanium dioxide nanoparticles (TiO_2 NPs), a mixture of silicon dioxide nanoparticles (SiO_2 NPs), and silver nanoparticles (Ag NPs), in the germination of *Z. mays* and *Glycine max* seeds [54,55]. In order to clarify this concept, these researches also proposed a possible mechanism for seed germination. It is commonly recognized that magnesium is a practically necessary macronutrient for plant growth and that its ions are crucial for the activation of enzymes that are involved in seed germination. It is thus envisioned that similar methods may be used in the context of MgO NPs [54–56]. In general, nanoparticles aid in raising the level of the enzyme nitrate reductase, which improves the seeds' capacity to absorb and use water and other nutrients [57]. Gibberellic acid (GA), which is present in the embryo, is dissolved by the water absorbed by seeds, travels through seed tissues to the aleuronic cytoplasm, It generates the enzyme amylase, which hydrolyzes the starch in seed to sugars (maltose), by giving seed cells the energy because they need to germinate [58,59]. This strengthens the antioxidant systems of seeds [60], as displayed above in the schematic illustration of potential putative pathways involved in the germination of maize seeds treated with MgO NPs. All of these modifications work together to improve maize seed germination.

4.3. Exposed to MgO NPs in Greenhouse

In this section of our experiment, seed germinated in the greenhouse was firstly placed in the control condition for three days. After three days of germination, the germinated seed hardened into the greenhouse openly for one month. MgO nanoparticles were sprayed

on the leaves after the interval of seven days. Using the same concentration of 1 mL for one plant, three replications were tested for each concentration to check the effect of MgO nanoparticles under greenhouse conditions. The data were collected after one month, and there was a remarkable change in roots' and shoots' elongation and height. Magnesium (Mg) is an essential nutrient for plants that is required for several physiological processes, including photosynthesis, enzyme activity, and overall plant growth. Recent agricultural research has shown interest in magnesium oxide nanoparticles (Mg+ NP) as a potential means of enhancing crop yield and plant development.

4.4. Exposure to MgO NPs in Field

For further study, an experiment was set in the field. *Z. mays* was sprayed on leaves with different concentrations of MgO NPs. A lasting solution to this issue is to enhance the nutritional content of maize, particularly by biofortification, given the correlation between high levels of malnutrition and maize intake in many low-income countries [61]. According to the results of the in-field investigation, maize treated with MgO NPs significantly accelerated in development when compared to control (untreated plants) and plants treated with the corresponding growth. Furthermore, it was noted that the enhancement of plant development depended on concentration.

4.5. Interpretation to MgO NPs in Biochemical Characterization

Proceeding towards biochemical characterization, we initially come to antioxidant enzyme superoxide dismutase activity (SOD), which catalyzes the dissociation of superoxide anion to produce H_2O_2 and O_2^- antioxidant enzyme [62]. MgO-treated seedlings have the highest SOD activity under 500 ppm concentration. A similar phenomenon occurs with catalysis of the oxidation of phenols and amines by hydrogen peroxide (POD), which has the dual effects of eliminating the toxicity of hydrogen peroxide and phenols and amines [63]. It is the most important H_2O_2 scavenging enzyme (CAT) and plays an important role in the active oxygen scavenging system [64]. The characteristic absorption peak of H_2O_2 and copper-containing oxidase can oxidize monobasic phenol (PPO) and dibasic phenol to produce quinone, which causes browning [65]. In measuring membrane lipid peroxidation, the amount of MDA can determine the degree of lipid oxidation. The most prevalent active oxygen molecule in living things is H_2O_2 , which is mostly created by SOD and XOD and broken down by POD and CAT [66]. In addition to being a significant reactive oxygen species, H_2O_2 serves as the center of the transition of reactive oxygen species. O_2^- is the primary reactive oxygen species that plants make during metabolism. The amount and pace of O_2^- production in plants have greatly risen, and this has the intensity of membrane lipid peroxidation [67]. The amount of soluble protein is used to determine the activity of an enzyme. Additionally, food and other quality analyses employ the soluble content [68]. Reduced monosaccharides in the sample, as well as sucrose, maltose, and starch that, in the circumstances of this procedure, can partially hydrolyze to glucose, are referred to as soluble sugar. Because of their great nutritional value and potential medical benefits, plant phenols are widely used in food, medicine, cosmetics, and other industries.

They also can scavenge free radicals and have anti-oxidant and anti-aging properties [69]. Protein content is a vital component of the system that controls reactive oxygen species. The enzymes' folding, stability, degradation, and activation are controlled by proteins, and these processes have significant effects on ROS buildup and plant stress tolerance [70]. Compression has shown that total phenols (TPs) are active during the process of plant growth and play a significant positive role in the plant growth mechanism [71]. In the total phenols, a higher MgO content also offers the greatest advantage. L-phenylalanine was converted by PAL to yield trans-carnosic acid, which was the form with the highest absorption rate. The Application was also tested with phenolics including tannins and flavonoid, which are types of plant polyphenol and secondary metabolites. Tannins possess distinct chemical properties and exhibit various physiological activities, Such as combining

with protein, alkaloid, and polysaccharide. On the other hand, flavonoids are known for their anti-inflammatory, antibacterial, and hypolipidemic properties. As well as their ability to scavenging hydroxyl radicals. AchE is a serine hydrolase, and AchE catalyzes the hydrolysis of acetylcholine (Ach) [43].

5. Conclusions

The extract of Gui hua (*Osmanthus fragrans*) was used to synthesize the MgO NPs that showed great potential. Some analysis tools, such as TEM, SEM, FTIR, XRD, zeta potential, and TG were applied to characterize the synthesized MgO nanoparticles systematically. The percentage of germination of the seeds was dramatically increased by the biologically produced MgO NPs. According to the current research, these nanoparticles can be utilized to disrupt seed dormancy and promote early germination of seeds. Furthermore, it was observed that MgO NP concentration enhanced the development of *Z. mays* seedlings cultivated in a greenhouse. When sprayed with NPs, they showed strong results in a greenhouse at intervals of seven days for a month. After the seedling growth, the results showed in favor of 500 ppm concentration in all physiological characterizations. Likewise, MgO NPs also have a great influence on plant growth and productivity promotion in the field. Good results were seen in plant color (green) due to amazing performance in Pn (photosynthesis). The AAS (atomic absorption spectroscopy) and characterization study confirm the results, as do the high MgO contents in leaves, roots, and seeds treated with 500 ppm concentration compared to control (CK). We also observed that the biologically synthesized nanoparticle assists their easy penetration and translocation in various plant parts. Thus, it is observed and concluded that treatment with MgO NPs helps to promote seed germination, seedling growth, and plant growth promotion. Hence, these MgO NPs can be efficaciously used as nano-nutrients for the promotion of more efficient plant growth. Substantial studies are required to exact translocation in further plant parts, and to understand the translocation at the molecular level. The influence of MgO NPs will be important to improve the health of food.

Author Contributions: Z.A. and W.H. conceived the research and designed the experiments. Z.A. performed research, analyzed the data, and wrote the manuscript. M.A.H. and M.X. participated in data summarization and helped with analysis. H.Y. and X.C. analyzed and interpreted the data. X.F. and L.L. modified the manuscript. All authors have read and agreed to the published version of the manuscript.

Funding: Anhui Provincial Science Foundation for Young Talents (gxyq2022055), and Talent Projects of Anhui Science and Technology University (NXYJ201602).

Institutional Review Board Statement: Not applicable.

Informed Consent Statement: Not applicable.

Data Availability Statement: Available on request.

Conflicts of Interest: The authors declare no conflicts of interest.

References

1. Ditta, A. How helpful is nanotechnology in agriculture? *Adv. Nat. Sci. Nanosci. Nanotechnol.* **2012**, *3*, 033002. [[CrossRef](#)]
2. Parisi, C.; Vigani, M.; Rodríguez-Cerezo, E. Agricultural Nanotechnologies: What are the current possibilities? *Nano Today* **2015**, *10*, 124–127. [[CrossRef](#)]
3. Kaul, R.K.; Kumar, P.; Burman, U.; Joshi, P.; Agrawal, A.; Raliya, R.; Tarafdar, J.C. Magnesium and iron nanoparticles production using microorganisms and various salts. *Mater. Sci.* **2012**, *30*, 254–258. [[CrossRef](#)]
4. Prasad, R.; Bhattacharyya, A.; Nguyen, Q.D. Nanotechnology in Sustainable Agriculture: Recent Developments, Challenges, and Perspectives. *Front. Microbiol.* **2017**, *8*, 1014. [[CrossRef](#)] [[PubMed](#)]
5. Appu, M.; Ramalingam, P.; Sathiyarayanan, A.; Huang, J. An overview of plant defense-related enzymes responses to biotic stresses. *Plant Gene* **2021**, *27*, 100302. [[CrossRef](#)]
6. Abdelghany, T.M.; Al-Rajhi, A.M.H.; Yahya, R.; Bakri, M.M.; Al Abboud, M.A.; Yahya, R.; Qanash, H.; Bazaid, A.S.; Salem, S.S. Phytofabrication of zinc oxide nanoparticles with advanced characterization and its antioxidant, anticancer, and antimicrobial activity against pathogenic microorganisms. *Biomass-Converts. Biorefinery* **2022**, *13*, 417–430. [[CrossRef](#)]

7. Al-Rajhi, A.M.; Salem, S.S.; Alharbi, A.A.; Abdelghany, T. Ecofriendly synthesis of silver nanoparticles using Kei-apple (*Dovyalis caffra*) fruit and their efficacy against cancer cells and clinical pathogenic microorganisms. *Arab. J. Chem.* **2022**, *15*, 103927. [[CrossRef](#)]
8. Mohamed, A.A.; Abu-Elghait, M.; Ahmed, N.E.; Salem, S.S. Correction to: Eco-Friendly Mycogenic Synthesis of ZnO and CuO Nanoparticles for In Vitro Antibacterial, Antibiofilm and Antifungal Applications. *Biol. Trace Elem. Res.* **2021**, *199*, 2800–2801. [[CrossRef](#)]
9. Shang, Y.; Hasan, M.K.; Ahammed, G.J.; Li, M.; Yin, H.; Zhou, J. Applications of Nanotechnology in Plant Growth and Crop Protection: A Review. *Molecules* **2019**, *24*, 2558. [[CrossRef](#)] [[PubMed](#)]
10. Leung, Y.H.; Ng, A.M.C.; Xu, X.; Shen, Z.; Gethings, L.A.; Wong, M.T.; Chan, C.M.N.; Guo, M.Y.; Ng, Y.H.; Djurišić, A.B.; et al. Mechanisms of Antibacterial Activity of MgO: Non-ROS Mediated Toxicity of MgO Nanoparticles Towards *Escherichia coli*. *Small* **2014**, *10*, 1171–1183. [[CrossRef](#)] [[PubMed](#)]
11. Di, D.-R.; He, Z.-Z.; Sun, Z.-Q.; Liu, J. A new nano-cryosurgical modality for tumor treatment using biodegradable MgO nanoparticles. *Nanomed. Nanotechnol. Biol. Med.* **2012**, *8*, 1233–1241. [[CrossRef](#)]
12. Patel, M.K.; Zafaryab; Alam Rizvi, M.M.; Agrawal, V.V.; Ansari, Z.A.; Malhotra, B.D.; Ansari, S.G. Antibacterial and Cytotoxic Effect of Magnesium Oxide Nanoparticles on Bacterial and Human Cells. *J. Nanoeng. Nanomanufacturing* **2013**, *3*, 162–166. [[CrossRef](#)]
13. Cai, L.; Liu, M.; Liu, Z.; Yang, H.; Sun, X.; Chen, J.; Xiang, S.; Ding, W. MgONPs Can Boost Plant Growth: Evidence from Increased Seedling Growth, Morpho-Physiological Activities, and Mg Uptake in Tobacco (*Nicotiana tabacum* L.). *Molecules* **2018**, *23*, 3375. [[CrossRef](#)]
14. Raliya, R.; Tarafdar, J.C.; Singh, S.K.; Gautam, R.; Choudhary, K.; Maurino, V.G.; Saharan, V. MgO Nanoparticles Biosynthesis and Its Effect on Chlorophyll Contents in the Leaves of Clusterbean (*Cyamopsis tetragonoloba* L.). *Adv. Sci. Eng. Med.* **2014**, *6*, 538–545. [[CrossRef](#)]
15. Khot, L.R.; Sankaran, S.; Maja, J.M.; Ehsani, R.; Schuster, E.W. Applications of nanomaterials in agricultural production and crop protection: A review. *Crop. Prot.* **2012**, *35*, 64–70. [[CrossRef](#)]
16. Sekhon, B. Nanotechnology in agri-food production: An overview. *Nanotechnol. Sci. Appl.* **2014**, *7*, 31–53. [[CrossRef](#)]
17. Siddiqui, M.H.; Al-Wahaibi, M.H.; Mohammad, F. *Role of Nanoparticles in Plants, in Nanotechnology and Plant Sciences: Nanoparticles and Their Impact on Plants*; Siddiqui, M.H., Al-Wahaibi, M.H., Mohammad, F., Eds.; Springer International Publishing: Cham, Switzerland, 2015; pp. 19–35.
18. Pugazhendhi, A.; Prabhu, R.; Muruganatham, K.; Shanmuganathan, R.; Natarajan, S. Anticancer, antimicrobial and photocatalytic activities of green synthesized magnesium oxide nanoparticles (MgONPs) using aqueous extract of *Sargassum wightii*. *J. Photochem. Photobiol. B Biol.* **2019**, *190*, 86–97. [[CrossRef](#)]
19. Chen, J.; Sun, L.; Cheng, Y.; Lu, Z.; Shao, K.; Li, T.; Hu, C.; Han, H. Graphene Oxide-Silver Nanocomposite: Novel Agricultural Antifungal Agent against *Fusarium graminearum* for Crop Disease Prevention. *ACS Appl. Mater. Interfaces* **2016**, *8*, 24057–24070. [[CrossRef](#)]
20. Horst, A.M.; Vukanti, R.; Priester, J.H.; Holden, P.A. An Assessment of Fluorescence- and Absorbance-Based Assays to Study Metal-Oxide Nanoparticle ROS Production and Effects on Bacterial Membranes. *Small* **2013**, *9*, 1753–1764. [[CrossRef](#)] [[PubMed](#)]
21. Kalhapure, R.S.; Suleman, N.; Mocktar, C.; Seedat, N.; Govender, T. Nanoengineered Drug Delivery Systems for Enhancing Antibiotic Therapy. *J. Pharm. Sci.* **2015**, *104*, 872–905. [[CrossRef](#)] [[PubMed](#)]
22. Singh, C.R. Review on Problems and its Remedy in Plant Tissue Culture. *Asian J. Biol. Sci.* **2018**, *11*, 165–172. [[CrossRef](#)]
23. Cai, L.; Chen, J.; Liu, Z.; Wang, H.; Yang, H.; Ding, W. Magnesium Oxide Nanoparticles: Effective Agricultural Antibacterial Agent Against *Ralstonia solanacearum*. *Front. Microbiol.* **2018**, *9*, 790. [[CrossRef](#)] [[PubMed](#)]
24. Shinde, S.; Paralikar, P.; Ingle, A.P.; Rai, M. Promotion of seed germination and seedling growth of *Zea mays* by magnesium hydroxide nanoparticles synthesized by the filtrate from *Aspergillus niger*. *Arab. J. Chem.* **2020**, *13*, 3172–3182. [[CrossRef](#)]
25. Guo, W.; Nazim, H.; Liang, Z.; Yang, D. Magnesium deficiency in plants: An urgent problem. *Crop. J.* **2016**, *4*, 83–91. [[CrossRef](#)]
26. Martínez-Mera, I.; Espinosa-Pesqueira, M.; Pérez-Hernández, R.; Arenas-Alatorre, J. Synthesis of magnetite (Fe₃O₄) nanoparticles without surfactants at room temperature. *Mater. Lett.* **2007**, *61*, 4447–4451. [[CrossRef](#)]
27. Camtakan, Z.; Erenturk, S.; Yusan, S. Magnesium oxide nanoparticles: Preparation, characterization, and uranium sorption properties. *Environ. Prog. Sustain. Energy* **2012**, *31*, 536–543. [[CrossRef](#)]
28. Sharma, G.; Soni, R.; Jasuja, N.D. Phytoassisted synthesis of magnesium oxide nanoparticles with *Swertia chirayaita*. *J. Taibah Univ. Sci.* **2017**, *11*, 471–477. [[CrossRef](#)]
29. Sushma, N.J.; Prathyusha, D.; Swathi, G.; Madhavi, T.; Raju, B.D.P.; Mallikarjuna, K.; Kim, H.-S. Facile approach to synthesize magnesium oxide nanoparticles by using *Clitoria ternatea*—characterization and in vitro antioxidant studies. *Appl. Nanosci.* **2016**, *6*, 437–444. [[CrossRef](#)]
30. Mast, J.; Verleysen, E.; Hodoroaba, V.D.; Kaegi, R. Chapter 2.1.2-Characterization of nanomaterials by transmission electron microscopy: Measurement procedures. In *Characterization of Nanoparticles*; Hodoroaba, V.-D., Unger, W.E.S., Shard, A.G., Eds.; Elsevier: Amsterdam, The Netherlands, 2020; pp. 29–48.
31. Pilarska, A.; Wysokowski, M.; Markiewicz, E.; Jesionowski, T. Synthesis of magnesium hydroxide and its calcinates by a precipitation method with the use of magnesium sulfate and poly(ethylene glycols). *Powder Technol.* **2013**, *235*, 148–157. [[CrossRef](#)]

32. Holder, C.F.; Schaak, R.E. Tutorial on Powder X-ray Diffraction for Characterizing Nanoscale Materials. *ACS Nano* **2019**, *13*, 7359–7365. [[CrossRef](#)]
33. Thakar, M.A.; Jha, S.S.; Phasinam, K.; Manne, R.; Qureshi, Y.; Babu, V.H. X ray diffraction (XRD) analysis and evaluation of antioxidant activity of copper oxide nanoparticles synthesized from leaf extract of *Cissus vitiginea*. *Mater. Today Proc.* **2022**, *51*, 319–324. [[CrossRef](#)]
34. Hirayama, T.; Mochida, K. Plant Hormonomics: A Key Tool for Deep Physiological Phenotyping to Improve Crop Productivity. *Plant Cell Physiol.* **2023**, *63*, 1826–1839. [[CrossRef](#)] [[PubMed](#)]
35. Rajput, V.D.; Harish; Singh, R.K.; Verma, K.K.; Sharma, L.; Quiroz-Figueroa, F.R.; Meena, M.; Gour, V.S.; Minkina, T.; Sushkova, S.; et al. Recent Developments in Enzymatic Antioxidant Defence Mechanism in Plants with Special Reference to Abiotic Stress. *Biology* **2021**, *10*, 267. [[CrossRef](#)]
36. Khalofah, A.; Migdadi, H.; El-Harty, E. Antioxidant Enzymatic Activities and Growth Response of Quinoa (*Chenopodium quinoa* Willd) to Exogenous Selenium Application. *Plants* **2021**, *10*, 719. [[CrossRef](#)]
37. Jha, Y.; Mohamed, H.I. Enhancement of disease resistance, growth potential, and biochemical markers in maize plants by inoculation with plant growth-promoting bacteria under biotic stress. *J. Plant Pathol.* **2023**, *105*, 729–748. [[CrossRef](#)]
38. Kumar, C.; Chand, P.; Choudhary, C.S.; Maurya, S.; Kumar, A.; Priya, S. Activity of different defense related antioxidative biochemical compound upon exogenous application of different elicitors on maize against *Helminthosporium maydis* Y. Nisik & C. Miyake. *Cereal Res. Commun.* **2023**, 1–11. [[CrossRef](#)]
39. Hasanuzzaman, M.; Inafuku, M.; Nahar, K.; Fujita, M.; Oku, H. Nitric Oxide Regulates Plant Growth, Physiology, Antioxidant Defense, and Ion Homeostasis to Confer Salt Tolerance in the Mangrove Species, *Kandelia obovata*. *Antioxidants* **2021**, *10*, 611. [[CrossRef](#)]
40. Mpanza, T.D.E.; Mani, S. Effects of Vachellia mearnsii Tannin Extract as an Additive on Fermentation Quality, Aerobic Stability, and Microbial Modulation of Maize Silage. *Microorganisms* **2023**, *11*, 2767. [[CrossRef](#)]
41. Yucharoen, R.; Srisuksomwong, P.; Julsrigival, J.; Mungmai, L.; Kaewkod, T.; Tragoolpua, Y. Antioxidant, Anti-Tyrosinase, and Anti-Skin Pathogenic Bacterial Activities and Phytochemical Compositions of Corn Silk Extracts, and Stability of Corn Silk Facial Cream Product. *Antibiotics* **2023**, *12*, 1443. [[CrossRef](#)]
42. Gao, J.; Zhang, Y.; Xu, C.; Wang, X.; Wang, P.; Huang, S. Abscisic acid collaborates with lignin and flavonoid to improve pre-silking drought tolerance by tuning stem elongation and ear development in maize (*Zea mays* L.). *Plant J.* **2023**, *114*, 437–454. [[CrossRef](#)]
43. Vivekanandhan, P.; Swathy, K.; Lucy, A.; Sarayut, P.; Patcharin, K. Entomopathogenic fungi based microbial insecticides and their physiological and biochemical effects on *Spodoptera frugiperda* (J.E. Smith). *Front. Cell. Infect. Microbiol.* **2023**, *13*, 1254475. [[CrossRef](#)]
44. Mihali, C.; Frumuzachi, O.; Nicolescu, A.; Babotă, M.; Păltinean, R.; Tanase, C.; Mocan, A. Valorization of Corn Silk as an Agricultural By-Product through the Optimization of Ultrasound-Assisted Extraction. *Appl. Sci.* **2024**, *14*, 1516. [[CrossRef](#)]
45. Henrist, C.; Mathieu, J.-P.; Vogels, C.; Rulmont, A.; Cloots, R. Morphological study of magnesium hydroxide nanoparticles precipitated in dilute aqueous solution. *J. Cryst. Growth* **2003**, *249*, 321–330. [[CrossRef](#)]
46. Susi, H. [17] The Strength of Hydrogen Bonding: Infrared Spectroscopy. In *Methods in Enzymology*; Academic Press: Cambridge, MA, USA, 1972; pp. 381–391.
47. Sheng, X.; Jiang, X.; Zhao, H.; Wan, D.; Liu, Y.; Ngwenya, C.A.; Du, L. FTIR study of hydrogen bonding interaction between fluorinated alcohol and unsaturated esters. *Spectrochim. Acta Part A Mol. Biomol. Spectrosc.* **2018**, *198*, 239–247. [[CrossRef](#)]
48. Guerin, A.C.; Riley, K.; Rupnik, K.; Kuroda, D.G. Determining the Energetics of the Hydrogen Bond through FTIR: A Hands-On Physical Chemistry Lab Experiment. *J. Chem. Educ.* **2016**, *93*, 1124–1129. [[CrossRef](#)]
49. Jeevanandam, J.; Chan, Y.S.; Danquah, M.K. Biosynthesis and characterization of MgO nanoparticles from plant extracts via induced molecular nucleation. *New J. Chem.* **2017**, *41*, 2800–2814. [[CrossRef](#)]
50. Fuliş, A.; Vlase, G.; Vlase, T.; Soica, C.; Heghes, A.; Craina, M.; Ledeti, I. Comparative kinetic analysis on thermal degradation of some cephalosporins using TG and DSC data. *Chem. Cent. J.* **2013**, *7*, 70. [[CrossRef](#)]
51. Da Costa, R.S.; Negrão, C.A.B.; Camelo, S.R.P.; Ribeiro-Costa, R.M.; Barbosa, W.L.R.; da Costa, C.E.F.; Silva Júnior, J.O.C. Investigation of thermal behavior of *Heliotropium indicum* L. lyophilized extract by TG and DSC. *J. Therm. Anal. Calorim.* **2013**, *111*, 1959–1964. [[CrossRef](#)]
52. Jayarambabu, N.; Kumari, S.B.; Rao, V.K.; Prabhu, Y.T. Enhancement of Growth In Maize By Biogenic- Synthesized Mgo Nanoparticles. *Int. J. Pure Appl. Zool.* **2016**, *4*, 262–270.
53. Segatto, C.; Souza, C.A.; Lajús, C.R.; Fiori, M.A.; Silva, L.L.; Riella, H.G.; Coelho, C.M.M. Pretreatment of maize seeds with different magnesium nanoparticles improves the germinating performance and storability. *Aust. J. Crop Sci.* **2020**, *14*, 1473–1478. [[CrossRef](#)]
54. Karunakaran, G.; Suriyaprabha, R.; Rajendran, V.; Kannan, N. Influence of ZrO₂, SiO₂, Al₂O₃ and TiO₂ nanoparticles on maize seed germination under different growth conditions. *IET Nanobiotechnol.* **2016**, *10*, 171–177. [[CrossRef](#)]
55. Almutairi, Z.; Alharbi, A. Effect of Silver Nanoparticles on Seed Germination of Crop Plants. World Academy of Science, Engineering and Technology. *Int. J. Biol. Biomol. Agric. Food Biotechnol. Eng.* **2015**, *4*, 280–285. [[CrossRef](#)]
56. Lu, C.; Zhang, C.; Wen, J.; Wu, G.; Tao, M. Research of the effect of nanometer materials on germination and growth enhancement of Glycine max and its mechanism. *Soybean Sci.* **2002**, *21*, 168–171.

57. Morales-Díaz, A.B.; Ortega-Ortíz, H.; Juárez-Maldonado, A.; Cadenas-Pliego, G.; González-Morales, S.; Benavides-Mendoza, A. Application of nanoelements in plant nutrition and its impact in ecosystems. *Adv. Nat. Sci. Nanosci. Nanotechnol.* **2017**, *8*, 013001. [[CrossRef](#)]
58. Biazus, J.P.M.; Santana, J.C.C.; Souza, R.R.; Tambourgi, E.B. Maximizing of production stages of malt from *Zea mays*. *Braz. J. Food Technol. Spec.* **2005**, 138–145. Available online: https://bjft.ital.sp.gov.br/especiais/ed_especial/24.pdf (accessed on 22 February 2024).
59. Biazus, J.P.M.; de Souza, R.R.; Márquez, J.E.; Franco, T.T.; Santana, J.C.C.; Tambourgi, E.B. Production and characterization of amylases from *Zea mays* malt. *Braz. Arch. Biol. Technol.* **2009**, *52*, 991–1000. [[CrossRef](#)]
60. Aslani, F.; Bagheri, S.; Julkapli, N.M.; Juraimi, A.S.; Hashemi, F.S.G.; Baghdadi, A. Effects of Engineered Nanomaterials on Plants Growth: An Overview. *Sci. World J.* **2014**, *2014*, 641759. [[CrossRef](#)] [[PubMed](#)]
61. Muleya, M.; Li, D.; Chiutsi-Phiri, G.; Botoman, L.; Brameld, J.M.; Salter, A.M. In vitro determination of the protein quality of maize varieties cultivated in Malawi using the INFOGEST digestion method. *Heliyon* **2023**, *9*, e19797. [[CrossRef](#)]
62. Stephenie, S.; Chang, Y.P.; Gnanasekaran, A.; Esa, N.M.; Gnanaraj, C. An insight on superoxide dismutase (SOD) from plants for mammalian health enhancement. *J. Funct. Foods* **2020**, *68*, 103917. [[CrossRef](#)]
63. Chen, Y.; Li, H.; Zhang, S.; Du, S.; Zhang, J.; Song, Z.; Jiang, J. Analysis of the main antioxidant enzymes in the roots of *Tamarix ramosissima* under NaCl stress by applying exogenous potassium (K⁺). *Front. Plant Sci.* **2023**, *14*, 1114266. [[CrossRef](#)]
64. Zeng, C.-Q.; Liu, W.-X.; Hao, J.-Y.; Fan, D.-N.; Chen, L.-M.; Xu, H.-N.; Li, K.-Z. Measuring the expression and activity of the CAT enzyme to determine Al resistance in soybean. *Plant Physiol. Biochem.* **2019**, *144*, 254–263. [[CrossRef](#)] [[PubMed](#)]
65. Zhang, S. Recent Advances of Polyphenol Oxidases in Plants. *Molecules* **2023**, *28*, 2158. [[CrossRef](#)] [[PubMed](#)]
66. Gomes, M.P.; Kitamura, R.S.A.; Marques, R.Z.; Barbato, M.L.; Zámocký, M. The Role of H₂O₂-Scavenging Enzymes (Ascorbate Peroxidase and Catalase) in the Tolerance of *Lemma minor* to Antibiotics: Implications for Phytoremediation. *Antioxidants* **2022**, *11*, 151. [[CrossRef](#)] [[PubMed](#)]
67. Zandi, P.; Schnug, E. Reactive Oxygen Species, Antioxidant Responses and Implications from a Microbial Modulation Perspective. *Biology* **2022**, *11*, 155. [[CrossRef](#)] [[PubMed](#)]
68. Bai, J.-H.; Liu, J.-H.; Zhang, N.; Yang, J.-H.; Sa, R.-L.; Wu, L. Effect of Alkali Stress on Soluble Sugar, Antioxidant Enzymes and Yield of Oat. *J. Integr. Agric.* **2013**, *12*, 1441–1449. [[CrossRef](#)]
69. Hou, P.; Wang, F.; Luo, B.; Li, A.; Wang, C.; Shabala, L.; Ahmed, H.A.I.; Deng, S.; Zhang, H.; Song, P.; et al. Antioxidant Enzymatic Activity and Osmotic Adjustment as Components of the Drought Tolerance Mechanism in *Carex duriuscula*. *Plants* **2021**, *10*, 436. [[CrossRef](#)]
70. Melicher, P.; Dvořák, P.; Šamaj, J.; Takáč, T. Protein-protein interactions in plant antioxidant defense. *Front. Plant Sci.* **2022**, *13*, 1035573. [[CrossRef](#)]
71. Luqman, M.; Shahbaz, M.; Maqsood, M.F.; Farhat, F.; Zulfiqar, U.; Siddiqui, M.H.; Masood, A.; Aqeel, M.; Haider, F.U. Effect of strigolactone on growth, photosynthetic efficiency, antioxidant activity, and osmolytes accumulation in different maize (*Zea mays* L.) hybrids grown under drought stress. *Plant Signal. Behav.* **2023**, *18*, 2262795. [[CrossRef](#)]

Disclaimer/Publisher’s Note: The statements, opinions and data contained in all publications are solely those of the individual author(s) and contributor(s) and not of MDPI and/or the editor(s). MDPI and/or the editor(s) disclaim responsibility for any injury to people or property resulting from any ideas, methods, instructions or products referred to in the content.